

RESEARCH ARTICLE

Cytochrome *c* Oxidase Biogenesis and Metallochaperone Interactions: Steps in the Assembly Pathway of a Bacterial Complex

Sonja Schimo¹*, Ilka Wittig²*, Klaas M. Pos^{1*}, Bernd Ludwig^{3*}

1 Institute of Biochemistry, Membrane Transport Machineries, Goethe-University, Frankfurt am Main, Germany, **2** Functional Proteomics, SFB 815 Core Unity, Faculty of Medicine, Goethe-University, Frankfurt am Main, Germany, **3** Institute of Biochemistry, Molecular Genetics, Goethe-University, Frankfurt am Main, Germany

* These authors contributed equally to this work.

* pos@em.uni-frankfurt.de (KMP); ludwig@em.uni-frankfurt.de (BL)



OPEN ACCESS

Citation: Schimo S, Wittig I, Pos KM, Ludwig B (2017) Cytochrome *c* Oxidase Biogenesis and Metallochaperone Interactions: Steps in the Assembly Pathway of a Bacterial Complex. *PLoS ONE* 12(1): e0170037. doi:10.1371/journal.pone.0170037

Editor: Alessandro Giuffrè, National Research Council, ITALY

Received: October 19, 2016

Accepted: December 27, 2016

Published: January 20, 2017

Copyright: © 2017 Schimo et al. This is an open access article distributed under the terms of the [Creative Commons Attribution License](https://creativecommons.org/licenses/by/4.0/), which permits unrestricted use, distribution, and reproduction in any medium, provided the original author and source are credited.

Data Availability Statement: All relevant data are within the paper and its Supporting Information files.

Funding: The project was funded by Deutsche Forschungsgemeinschaft (DFG, www.dfg.de) DFG Grant numbers LU 318/5-1: to BL, SFB815, project Z1: to IW, PO 1344/3-1) to KMP. The funder had no role in study design, data collection and analysis, decision to publish, or preparation of the manuscript.

Abstract

Biogenesis of mitochondrial cytochrome *c* oxidase (COX) is a complex process involving the coordinate expression and assembly of numerous subunits (SU) of dual genetic origin. Moreover, several auxiliary factors are required to recruit and insert the redox-active metal compounds, which in most cases are buried in their protein scaffold deep inside the membrane. Here we used a combination of gel electrophoresis and pull-down assay techniques in conjunction with immunostaining as well as complexome profiling to identify and analyze the composition of assembly intermediates in solubilized membranes of the bacterium *Paracoccus denitrificans*. Our results show that the central SUI passes through at least three intermediate complexes with distinct subunit and cofactor composition before formation of the holoenzyme and its subsequent integration into supercomplexes. We propose a model for COX biogenesis in which maturation of newly translated COX SUI is initially assisted by CtaG, a chaperone implicated in Cu_B site metallation, followed by the interaction with the heme chaperone Surf1c to populate the redox-active metal-heme centers in SUI. Only then the remaining smaller subunits are recruited to form the mature enzyme which ultimately associates with respiratory complexes I and III into supercomplexes.

Introduction

The heme *aa*₃-type cytochrome *c* oxidase (COX) is the terminal electron acceptor in the respiratory chain of mitochondria and many bacteria. It catalyzes the transfer of electrons from cytochrome *c* to molecular oxygen, a reaction that is coupled to the translocation of protons across the membrane. It thus contributes to the generation of a proton gradient, which is subsequently used to drive ATP synthesis [1, 2]. The mitochondrial enzyme consists of up to 13 different subunits (SU), with three highly conserved core SU I-III [3, 4] which are encoded by the organellar genome and represent the minimal functional entity in most bacterial oxidases as well. As the main catalytic player, COX SUI houses both the heme moieties (*a* and *a*₃) and a

Competing Interests: The authors have declared that no competing interests exist.

Abbreviations: BN, blue native; Co-IP, co-immunoprecipitation; complex I, NADH:ubiquinone oxidoreductase; complex III, ubiquinol:cytochrome *c* oxidoreductase; complex V, ATP synthase; COX, cytochrome *c* oxidase or complex IV; cyt *c*₅₅₂, cytochrome *c*₅₅₂; DDM, *n*-dodecyl- β -D-maltoside; DSP, dithiobis(succinimidyl)propionate; IBAQ, intensity-based absolute quantification; MS, mass spectrometry; PAGE, polyacrylamide gel electrophoresis; SU, subunit; WT, wildtype.

copper ion (Cu_B), which are located by one third into the depth of the membrane. SUII carries two copper ions in a mixed valence state, constituting the Cu_A center; it serves as the first entry point for the electron which is further shuttled to heme *a* and then to the heme *a*₃-Cu_B binuclear center, where oxygen is reduced to water.

Biogenesis of this multi-subunit and multi-cofactor enzyme is a highly complex process in mitochondria, involving the coordinated expression of subunits derived from two compartmentally separated genomes, their import into the mitochondrion as well as their assembly into the holoenzyme, strictly dependent also on the synthesis, recruitment and insertion of redox-active cofactors [5–9]. Studies to understand these processes in detail and to sequentially follow those steps have suggested that COX assembly is initiated with COX SUI as a nucleation point and proceeds with the formation of distinct assembly intermediates [9, 10]. Most of these steps are assisted by assembly factors, ensuring proper progression towards a functional, correctly assembled protein complex. A majority of these chaperones has been identified by systematic analysis of COX biogenesis defects in *Saccharomyces cerevisiae*, revealing more than 30 such auxiliary proteins [8, 11]. However, many of these are implicated in transcriptional and translational regulation or involved in early assembly steps, often poorly conserved between higher eukaryotes [12, 13]. Among the assembly factors with the highest degree of sequence conservation are those involved in the synthesis or incorporation of cofactors, some of them are even part of the terminal oxidase operon in bacteria [14, 15], emphasizing their importance and suggesting that the core assembly processes share still today, from bacteria to eukaryotes, similar mechanistic features.

Focussing on the metallation of COX SUI, it is worth mentioning that heme *a* is an exclusive cofactor of terminal oxidases. This cofactor is synthesized in two steps from heme *b* in the mitochondrion, involving two membrane-bound enzymes. First, heme *o* synthase (Cox10 in eukaryotes, CtaB in prokaryotes) transfers a farnesyl diphosphate to heme *b* [16], which is subsequently oxidized by heme *a* synthase (Cox15 in eukaryotes, CtaA in prokaryotes) to form heme *a* [17]. Whilst heme *a* biosynthesis is essential for COX assembly [18, 19], the exact mechanism of cofactor insertion and players involved remains unresolved. A recent study in mitochondria suggests that oligomerization of Cox15 may be important for both heme *a* biosynthesis and subsequent delivery to maturing COX [20], as Cox15 has also been found to be associated with Cox SUI containing assembly intermediates and with the assembly factor Shy1p (Surf1c in prokaryotes; [21]). The latter is a well-known COX biogenesis factor, whose functional loss is connected to Leigh syndrome in humans, a severe neurodegenerative disorder [22–24]. Even though the yeast homologue Shy1p is one of the best studied Surf1 homologues and found to interact with COX assembly intermediates [21, 25–27], studies in bacteria established its role as a heme *a* binding protein and its involvement in the hemylation of COX SUI [14, 28, 29].

The Cu_B site formation in COX SUI is dependent on the assembly factor Cox11 (termed CtaG in prokaryotes), substantially supported by studies in *Rhodobacter sphaeroides* and *S. cerevisiae* [30–32]. Recently, a physical association of CtaG and COX SUI was confirmed in *Paracoccus denitrificans* [33].

The Sco proteins Sco1 and Sco2 are implicated in the metallation of the Cu_A center in COX SUII. Whilst Sco1 is generally accepted to play an active role in this process since a direct interaction with SUII was confirmed in both yeast and mammalian cells [34–38], the ultimate function of Sco2 is still under debate. In humans Sco2 may act as a thiol-disulfide oxidoreductase for Sco1 and thus is indirectly involved in the maturation of SUII [39, 40].

Bacterial oxidases are far simpler in structure compared to their mitochondrial counterparts, comprising only a basic set of subunits whose expression and assembly is dependent on a single genetic system and a limited number of key biogenesis factors. Therefore, *P.*

denitrificans, one of the closest evolutionary relatives to present-day mitochondria [41], is a well-suited model to study fundamental processes of COX biogenesis.

Here we present additional insight into the assembly pathway of maturing bacterial cytochrome *c* oxidase and its interplay with COX specific metallochaperones. Blue native electrophoresis in combination with either Western blot analysis or complexome profiling and pull-down assays allow us to identify and characterize the composition of four distinct COX SUI assembly intermediates. Our data suggest an early association of this subunit with CtaG, followed by the interaction with Surf1c, the subsequent association with SUII, III and IV, and the final insertion of the holoenzyme into respiratory supercomplexes.

Materials and Methods

Chemicals

n-dodecyl- β -D-maltoside (DDM; >99.5%) was purchased from GLYCON Biochemicals (Luckenwalde, Germany) and digitonin (99.9%) from Roth (Karlsruhe, Germany). Protein A/G-coated magnetic beads, the PageRuler prestained protein ladder #26616 and the amine-reactive crosslinker dithiobis(succinimidyl) propionate (DSP) were purchased from Thermo Scientific (Waltham, MA, USA).

Paracoccus denitrificans strains

The parental strain used in this study was Pd1222 (DSM413 derivative, Rif^r, Sp^r, enhanced conjugation frequencies, m⁻; [42]). In strain FA2 (Pd1222, $\Delta surf1c::Kan^r$, Rif^r; [15]) the *surf1c* gene was replaced by a kanamycin resistance cassette introduced by homologous recombination. Both alleles of cytochrome *c* oxidase subunit I are replaced in strain MR31 (Pd1222, $\Delta ctaDI::Km^r$, $\Delta ctaDII::Tc^r$; [43]) by kanamycin and tetracycline resistance genes. In strain ST4 ($\Delta cta::neo$) most of the *cta* operon from *ctaC* to *ctaE* was replaced by a kanamycin resistance gene [44], see also Table 1.

In vivo crosslinking of intact cells, and membrane preparation

P. denitrificans cultures were grown to exponential phase and washed cells were crosslinked essentially as in [33] with DSP at a final concentration of 1 mM. Cells were disrupted using a Constant System cell disrupter (Constant Systems Ltd) at 1.85 kbar, followed by membrane preparation as described previously [28]. The protein concentration was determined using a modified Lowry protocol [45, 46].

Blue native gel electrophoresis

For blue native polyacrylamide gel electrophoresis (BN-PAGE) untreated membranes were solubilized with digitonin, mixed with appropriate loading buffer and applied to a 3.5–18% gradient BN gel (140 μ g protein per lane) with dimensions of 0.07 x 8.3 x 7.3 cm, essentially as described in [47]. For second-dimension SDS-PAGE, lanes were cut out, incubated in 1% SDS

Table 1. Genotype and sources of *P. denitrificans* strains.

Strain	Genotype	Strain description	source
Pd1222	DSM413 derivative, Rif ^r , Sp ^r , enhanced conjugation frequencies, m ⁻	WT	[42]
FA2	Pd1222, $\Delta surf1c::Kan^r$, Rif ^r	deletion of Surf1c gene	[15]
MR31	Pd1222, $\Delta ctaDI::Km^r$, $\Delta ctaDII::Tc^r$	deletions of both COX SUI genes	[43]
ST4	$\Delta ctaCBGE::Km^r$	large deletion affecting COX SUII, SUIII, CtaB and CtaG	[44]

doi:10.1371/journal.pone.0170037.t001

for 10 min at room temperature and run on a 10% SDS Tricine gel [48]. The separated complexes were either analyzed by silver-staining or by immunoblotting [28].

For complexome profiling, BN-PAGE was performed alike, employing a 3–18% BN gradient gel [47] with dimensions of 0.16 x 14 x 14 cm. As native protein standard, digitonin-solubilized bovine heart mitochondria were used [49].

Complexome profiling and data analysis

Complexome profiling (quantitative mass spectrometry) was performed essentially as described [50, 51] with the following modifications: peptides were loaded on a C18 reversed-phase precolumn (Zorbax 300SB-C18, Agilent Technologies) followed by separation on in-house packed 2.4 μ m Reprosil C18 resin (Dr. Maisch GmbH) picotip emitter tip (diameter 100 μ m, 15 cm long, New Objectives) using a gradient from mobile phase A (4% acetonitrile, 0.1% formic acid) to 30% mobile phase B (80% acetonitrile, 0.1% formic acid) for 20 min followed by a second gradient to 70% mobile phase B with a flow rate of 300 nl/min. Reference proteome set of *P. denitrificans* Uniprot (Download November 2015, 5019 entries) was used to identify peptides and proteins with a false discovery rate (FDR) of 1%.

Abundance profiles were generated by NOVA software [52] using intensity-based absolute quantification (IBAQ) values from MaxQuant. IBAQ values of proteins from gel lane fractions were normalized to maximum appearance.

Bovine heart mitochondria were used as mass ladder [53]. The corresponding slice number of the maximum appearance of mitochondrial complex IV (210 kDa), complex III dimer (480 kDa), complex V (620 kDa), complex I (1000 kDa) and respiratory supercomplex containing complex I, III dimer and one copy of complex IV (1650 kDa) was used for mass calibration. The equation [$f(x) = 18228 \cdot e^{(0.1076x)}$, $R^2 = 0.9848$] obtained by exponential regression was used to calculate the native masses of each slice.

Immunoprecipitation using magnetic beads

In case of untreated membranes (non-crosslinked), digitonin was used at a detergent/protein ratio of 8 g/g to solubilize 5 mg of membranes in 0.5 ml of 50 mM Tris/HCl (pH 7.2) for 1 h at 4°C. Crosslinked membranes were solubilized with DDM (detergent to protein ratio of 2 g/g) and cleared by ultracentrifugation at 100 000 x g for 1 h and 4°C. A suspension of protein A/G magnetic beads (25 μ l) was washed with buffer (20 mM Tris/HCl pH 7.2, 0.08% digitonin for untreated membranes; 20 mM Tris/HCl pH 7.2, 0.02% DDM for crosslinked membranes), incubated for 1 h at room temperature with antiserum for immunoprecipitation and subsequently incubated with the clarified solubilisate (1 h, room temperature). Unbound material was separated, using a magnetic stand, and beads were washed twice with 0.5 ml IP buffer (20 mM Tris/HCl pH 7.2, 50 mM NaCl, 0.08% digitonin for untreated membranes; 20 mM Tris/HCl pH 7.2, 150 mM NaCl, 0.02% DDM in case of crosslinked membranes), followed by the elution of bound proteins in 100 μ l 0.1 M glycine (pH 2) and immediate neutralization with 50 mM Tris/HCl (pH 7.5). As control unrelated antiserum was used. The eluted fractions were separated by 12% SDS PAGE and subsequently analyzed by immunoblotting.

Western blot analysis

For immunostaining, proteins were transferred to nitrocellulose membrane and treated with rabbit anti-COX (mainly recognizing COX SUI and II; [33]), anti-CtaG [33], anti-Surf1c or anti-CtaA antisera according to standard procedures; for detection, protein A alkaline phosphatase (Merck, Darmstadt, Germany) was used. The specificity of the employed antisera is documented in the S2 Fig.

Results

Biogenesis of cytochrome *c* oxidase is a highly complex process, involving both the recruitment of subunits as well as the incorporation of redox cofactors delivered by specific chaperones. We used two independent detection methods, immunostaining and mass spectrometry (MS), to identify intermediary assembly complexes during biogenesis of the heme *aa*₃-type terminal oxidase in *P. denitrificans*. First protein interactions were probed by two-dimensional gel electrophoresis and immunoprecipitation and further analyzed by complexome profiling, providing insight on additional COX biogenesis factors and their roles in the assembly process.

COX assembly intermediates and interacting metallochaperones detected by immunostaining

Membranes from *P. denitrificans*, prepared from wildtype (WT) and deletion strain cells, were solubilized with the mild detergent digitonin and separated in the first dimension by BN-PAGE, ensuring the preservation of weak protein-protein-interactions. A subsequent denaturing SDS-PAGE run in the second dimension was followed by Western blotting and used for the analysis of interacting components from the first dimension gel. Western blots were probed with antibodies directed against COX (recognizing mainly SUI and SUII), CtaG, Surf1c and CtaA.

Staining of COX SUI (Fig 1A) shows four distinct spots with approximate sizes of 100 (I₁), 140 (I₂), 200 (I₃) and 300 (I₄) kDa, revealing well-defined COX subassemblies, see below. Co-migration of COX SUII is observed first on the level of subassemblies I₂ and more dominant on I₃, suggesting a late entry point into the assembly line. Both COX SUI and SUII are also found in the three distinct supercomplexes at 900 (S_c), 1200 (S_b) and 1900 (S_a) kDa as previously reported [49]. These supercomplexes are associations of oxidase with either respiratory complex III and cytochrome *c*₅₅₂ (S_c: III₄IV₂, S_b: III₄IV₄) or of complex III, complex I and cyt *c*₅₅₂ (S_a: I₁III₄IV₄; S1, S3 and S4 Figs). Upon deletion of both COX SUI gene loci (MR31, deletions in *ctaDI/DII*; see Table 1) supercomplex formation is severely impaired and SUII is found spread from the low to the high molecular weight region (Fig 1B and S1, S3 and S4 Figs).

The copper chaperone CtaG is generally believed to mediate copper transfer into COX SUI [7]. Our data show two well-defined spots in the first dimension between around 60 and 120 kDa for CtaG (Fig 1A). We assume that the first spot (60–80 kDa) represents a higher homooligomeric state of CtaG (monomer 21.4 kDa; [12, 54]), since under normal growth conditions, only a minority of this chaperone should be actively engaged in interactions with newly synthesized COX subunits. Thus, this low molecular band may correspond to “idling” CtaG chaperone copies, whereas the second signal at higher molecular weight reveals a co-migration of the CtaG with the 62.4 kDa SUI (COX subcomplex I₁, dotted line a) and may hint at a genuine interaction between the chaperone and this oxidase subunit. To further support this observation, we analyzed the CtaG migration behaviour in an oxidase SUI deletion strain, demonstrating a clear shift of relative staining intensity towards the low molecular weight signal (Fig 1B). Additionally, staining of CtaG is also observed at higher molecular weight between 200 and 500 kDa (see Fig 1A) and even more pronounced in either mutant background (Fig 1B and 1C), hinting at associations of CtaG in complexes, even then the target subunit is missing.

The chaperone Surf1c is implicated in the insertion of heme into COX SUI [29]. Fig 1A shows two distinct spots at approximately 70 kDa and with higher staining intensity between 150 and 200 kDa. Similarly as for CtaG, we interpret the lowest molecular weight signal as the

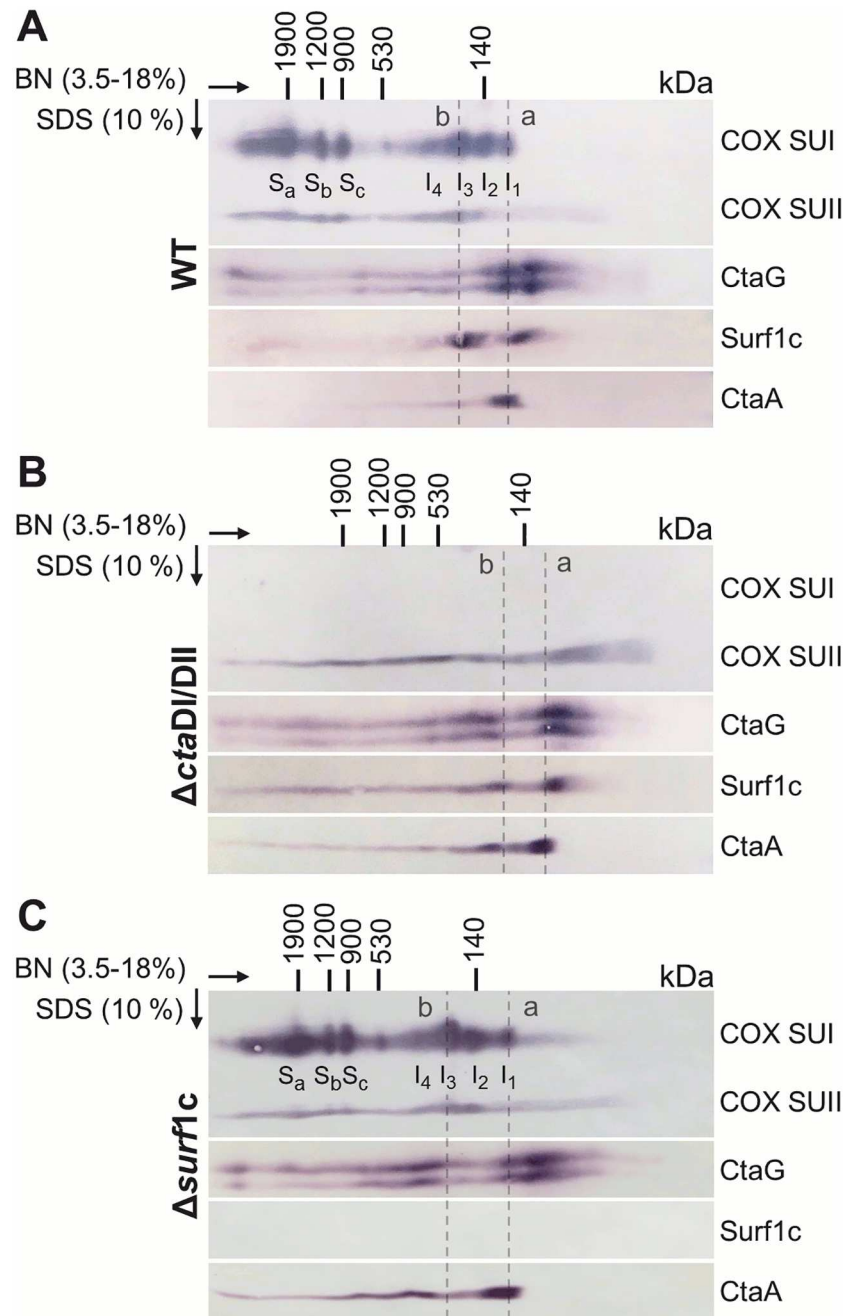


Fig 1. Two-dimensional BN/SDS-PAGE and Western blot analysis of COX assembly complexes. 140 μ g membranes prepared from *P. denitrificans* cells from strains (A) WT, (B) MR31 (Δ ctaD/DII), (C) FA2 (Δ surf1c) were solubilized with digitonin at a detergent/protein ratio of 4 g/g and subjected to a first dimension 3.5–18% gradient BN-PAGE. A gel strip was excised, soaked in 1% SDS and placed on top of a 10% SDS Tricine gel for separation in the second dimension. Proteins were transferred to a nitrocellulose membrane and analyzed by Western blotting with polyclonal antibodies directed against COX (recognizing SUI and SUII), CtaG, Surf1c or CtaA. To fully ascertain the positional alignment between different Western blots, critical blots were either re-stained with a second antibody of interest, or initially developed with a mixture of different antibodies (not shown). The approximate molecular masses have been assigned based on a molecular weight marker control and a previous mass estimation for molecular complexes in *P. denitrificans* [49]. The positions of the COX SUI subassemblies I₁₋₄ as well as the three supercomplexes S_{a-c} (nomenclature as in [49]) are indicated. In (A) the dotted line a shows COX SUI (62.4 kDa) and CtaG (21.4 kDa; known to migrate as double band on SDS PAGE [33]) on a vertical, whereas line b marks co-migration of COX SUI, SUII (28 kDa), CtaG, Surf1c (24.6 kDa) and less prominently of CtaA (41.8 kDa); in panel B these

assembly complexes are not observed, however the position of lines a and b is maintained as in (A) and (C) for comparison purposes.

doi:10.1371/journal.pone.0170037.g001

“idling” portion of Surf1c which is not actively involved in oxidase biogenesis interactions. The higher molecular weight spot coincides with COX-subcomplex I₃ and is significantly diminished in the oxidase SUI deletion strain (Fig 1B), hinting at an association between COX SUI and Surf1c (monomer 24.6 kDa); at the same time, this observation would also suggest that a COX chaperone biogenesis complex may exist to some extent (see Discussion) even when the target subunit is missing. Further, this same subassembly I₃, running in the first dimension at approximately 200 kDa, comprises distinct signals for COX SUII (28 kDa) and CtaG (21.4 kDa) as indicated by the dashed line b. Upon deletion of Surf1c (Fig 1C), we find that COX SUI, SUII and CtaG distribute very similarly in the first dimension gel, including the supercomplexes S_{a-c}.

The membrane-bound enzyme CtaA catalyzes the final step in the formation of heme *a*, a redox-active cofactor found exclusively in terminal oxidases [55]. We therefore asked whether CtaA may play a pivotal role in oxidase assembly as well. For CtaA in a WT background we observe one dominant band migrating in the first dimension at approximately 90–120 kDa and most probably representing a higher oligomeric state of CtaA (monomer 41.8 kDa; [20]). A second, weaker signal is detected at higher molecular weight at approximately 200 kDa, which becomes more dominant in both the Surf1c and oxidase SUI deletion strains and may hint at associations with oxidase subunits or other COX assembly factors.

Taken together, we present a likely sequence of events for the maturation of SUI, as represented by subcomplexes I₁ to I₄, showing both the interactions with metallochaperones and the entry of further COX subunits.

Direct interaction between oxidase and assembly factors Surf1c and CtaG

To further support the association of Surf1c, CtaG and CtaA with oxidase assembly intermediates, we performed a series of co-immunoprecipitations (co-IP), employing anti-COX, anti-CtaG, anti-Surf1c and anti-CtaA as bait antibodies and unrelated serum as control. Membranes were either prepared from exponentially growing untreated (non-crosslinked) cells or cells that were additionally crosslinked with DSP *in vivo* to covalently stabilize transient protein interactions. For each set of membranes, prepared from WT or deletion strains, pull-downs were conducted in parallel, incubating solubilized membranes with antibody-coated protein A/G magnetic beads. Beads were washed carefully to remove unspecific associations, specifically bound proteins were eluted with glycine (pH 2), immediately neutralized, and analyzed by Western blotting.

Fig 2 shows that all bait antibodies efficiently precipitate their respective target protein as expected. Using anti-COX as bait antibody (Fig 2, WT), not only COX subunits are pulled out, but also CtaG (as previously shown [33]) and, moreover, Surf1c. The reciprocal IP confirms these results, demonstrating for the first time a direct interaction between Surf1c and oxidase in the bacterial model system. Interestingly, the interaction between oxidase and the COX SUI specific Cu_B metallochaperone CtaG, is not exclusively mediated by COX SUI, but to some extent also by COX SUII, as documented in the oxidase SUI deletion strain. Furthermore, the association between CtaG and oxidase is independent of the heme chaperone Surf1c (Fig 2, FA2), however immunoprecipitation of Surf1c led to the co-IP of limited quantities of CtaG, and *vice versa*, indicating that these two proteins do interact with each other (Fig 2, WT).

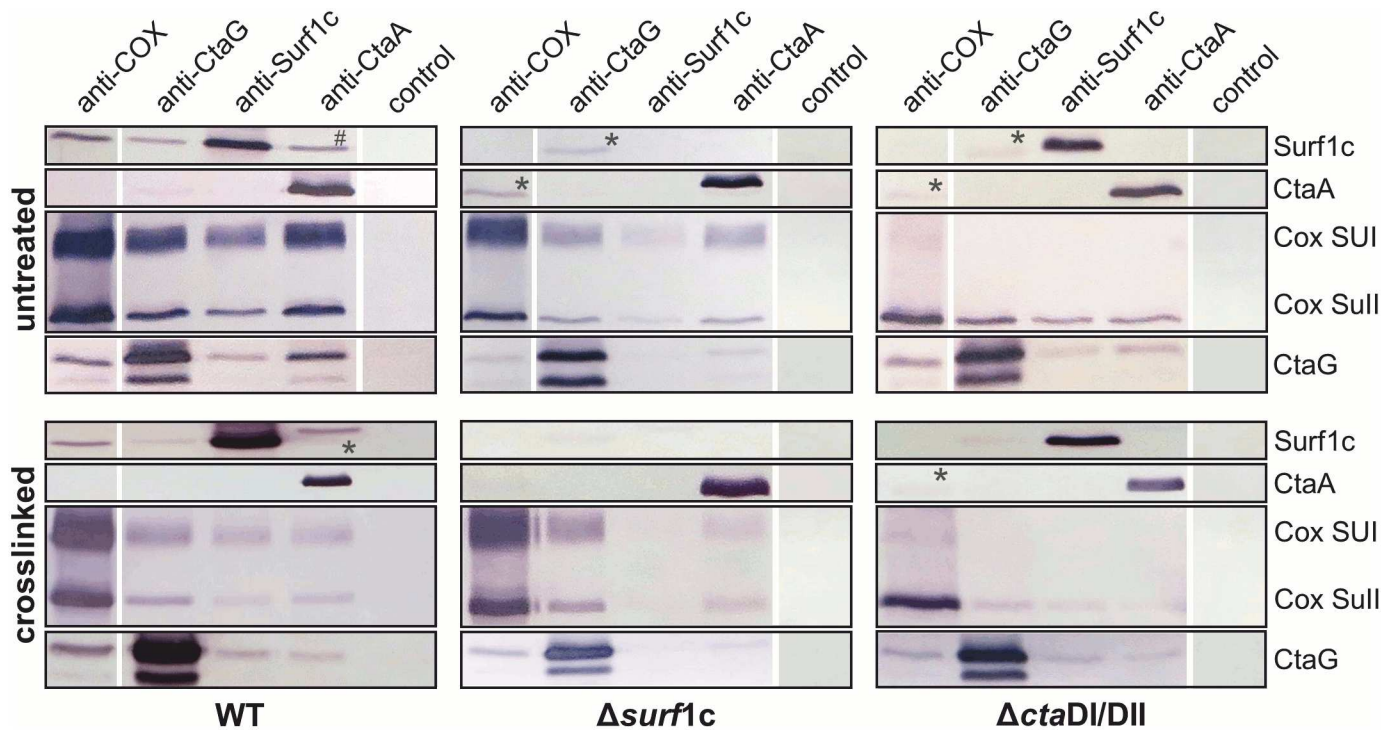


Fig 2. Pull-down assays indicating interactions between COX, Surf1c and CtaG. Interactions between COX, Surf1c, CtaG and CtaA were assayed by immunoprecipitation and subsequent Western blot analysis. Solubilized membranes from untreated (top) or crosslinked cells (bottom), including WT and deletion strains FA2 ($\Delta surf1c$) and MR31 ($\Delta ctaDI/DII$), were used for Co-IP experiments with protein A/G magnetic beads, as described in the experimental procedures. Eluates were separated by 12% SDS PAGE, blotted and probed against Surf1c, CtaA, COX SUI, COX Sull and CtaG. As bait antibody anti-COX (recognizing SUI and II), anti-CtaG, anti-Surf1c, anti-CtaA or a control serum was employed. The hashtag indicates a non-reproducible interaction and the asterisk designates unspecific staining (different molecular weight bands compared to control).

doi:10.1371/journal.pone.0170037.g002

The reciprocal interactions observed between oxidase and its assembly chaperones were further confirmed by *in vivo* crosslinking (Fig 2, crosslinked). This approach allows to covalently stabilize genuine protein interactions and to challenge isolated membranes in a much more stringent way during solubilization of membranes and in all subsequent washing steps, employing the more efficient detergent DDM instead of the rather mild detergent digitonin. Signals for the crosslinked samples are generally weaker, since chemical crosslinking as such and in particular in intact cells is not very efficient. Hence, under these harsher experimental conditions, yields for interacting complexes are lower.

For heme *a* synthase CtaA, there is no clear indication for either an association with oxidase or with the COX assembly factors CtaG and Surf1c. Even though Co-IP of COX or CtaG with CtaA is shown, the reciprocal experiment does not confirm this interaction.

Extending our view using a combined BN-PAGE-MS approach

Complexome profiling combines the advantages of BN-PAGE analysis, separating native protein complexes at high resolution, with MS for the identification of the underlying protein complexes and subunits [50]. In this study we used this method as a complementary approach to map COX assembly intermediates. After separation of digitonin-solubilized membranes by BN-PAGE, the gel was cut into 60 slices, subjected to in-gel trypsin digestion, followed by nano liquid chromatography-MS. A heat map illustration of selected proteins and corresponding migration profiles confirmed our previous finding that COX SUI is found in four distinct

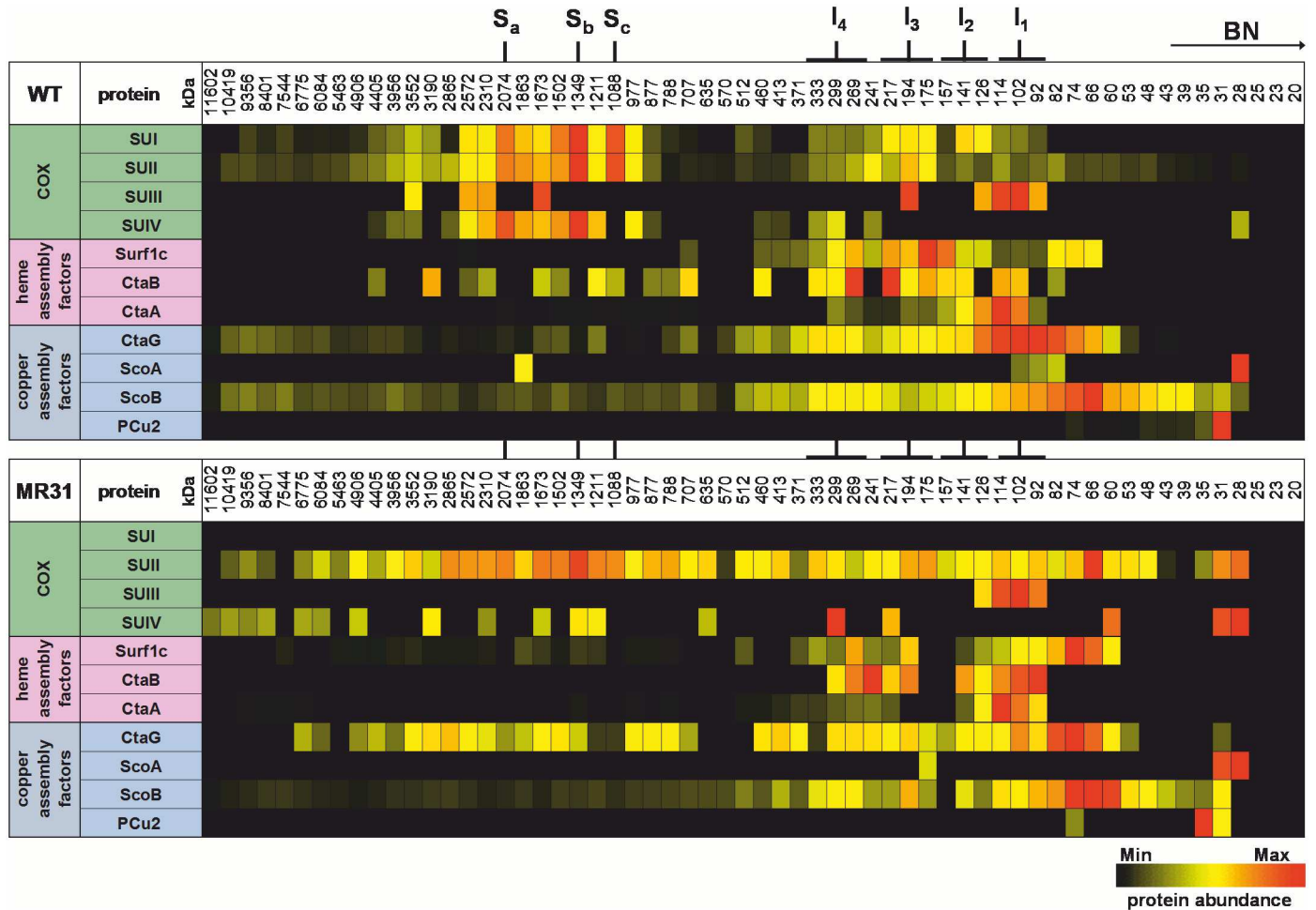


Fig 3. Heat map illustration of COX subunits and biogenesis factors identified by complexome profiling. 140 μ g of membranes prepared from WT (top panel) or oxidase SUI double deletion strain MR31 ($\Delta ctaDI/DII$; lower panel) were solubilized with detergent (digitonin:protein 2:1), separated by BN-PAGE and subsequently analyzed by quantitative MS. The position of supercomplexes (S_{a-c}) and COX SUI assembly intermediates (I_{1-4}) is indicated. For each identified protein, the data are normalized to maximum appearance over all 60 gel slices in each sample.

doi:10.1371/journal.pone.0170037.g003

assembly intermediates (I_1 - I_4 ; Figs 3 and 4A). Additionally, we find that both SUII (28 kDa) and SUIII (30.8 kDa) enter the assembly line only at the stage of subcomplex I_3 , and assume this latter SU to also populate I_4 as well. Due to its high hydrophobicity often leading to recovery problems [51] on the one hand, and the low overall protein amounts found for I_4 , we may fall below the detection limit here (see Figs 1A and 3A). SUIII is also found between 90 and 120 kDa in WT and in the oxidase SUI deletion strain; however, this position may represent only a storage pool of newly synthesized oligomeric SUIII.

Co-migration of SUIV with the COX core complex is observed shortly after the formation of subassembly I_3 at approximately 240 kDa and more dominantly at 300 kDa, corresponding to subcomplex I_4 . Interestingly, the largest proportion of COX subunits is found in the supercomplexes S_c , S_b and S_a . Consistent with our previous results supercomplex formation is lost altogether in the MR31 strain [49] but also in strain ST4 ($\Delta ctaCBGE::Km^r$; [44]), which carries, amongst others, deletions in the structural genes for SUII and SUIII, but was previously characterized to lack the SUI protein as well (Fig 3 and S1, S3 and S4 Figs).

Concerning the COX specific copper assembly factors, the complexome analysis shows co-migration of CtaG with COX SUI subcomplex I₁ and to a minor extent with the subassemblies I₂-I₄. In the absence of COX SUI a clear shift of CtaG migration behaviour is observed from approximately 100 kDa (I₁) to 75 kDa (Figs 3 and 4B), supporting our previous finding of an early association of CtaG with COX SUI. The *P. denitrificans* copper chaperone ScoB is the main player in the metallation of the Cu_A site of COX SUII [56]. ScoB (monomer 22.6 kDa) is widely distributed, with the highest proportion migrating at 66 kDa, which could be a complex of dimeric ScoB and COX SUII (28 kDa). This notion is supported by the dominant migration behaviour at around 66 kDa of COX SUII in the oxidase SUI deletion strain (Fig 3) and may hint to COX SUII being metallated prior to association with COX SUI.

For the proteins involved in heme *a* synthesis and hemylation of COX SUI our complexome data show migration of heme *a* synthase CtaA between 90 and 140 kDa. A similar distribution of CtaA is found in the MR31 and ST4 strains (Fig 3 and S3 Fig), suggesting that CtaA may be present in a higher homo-oligomeric state (see [20]) or at least not distinctly associated with COX SUI (Fig 3). In contrast, for Surf1c a clear association with subcomplex I₂ and I₃ is observed, where the strongest signal is visible at around 165 kDa, a position where COX SUII and SUIII do not yet interact with SUI. These Surf1c signals are lost in the absence of COX SUI (strain MR31, Δ ctaDI/DII), and Surf1c dominantly migrates at lower molecular weight between 60 and 80 kDa (Figs 3 and 4C).

Discussion

Defects in the biogenesis pathway of mitochondrial COX are associated with severe respiratory deficiencies. Distinct stages are passed during assembly of this multisubunit enzyme, involving both the timely association of subunits as well as the integration of their crucial redox-active metal centers. In eukaryotes more than 30 auxiliary factors have been identified that assist the expression and assembly process, of which only a limited set is conserved in bacteria such as *P. denitrificans*, where they are mainly implicated in either cofactor synthesis or delivery [7, 12, 13, 57]. So far, however, a comprehensive understanding of the sequential assembly steps and of cofactor incorporation is still lacking. In this study we focus on the identification of intermediary COX assembly states towards a functional holoenzyme using the bacterium *P. denitrificans* as a model system. Based on our data, we suggest a scenario for a sequential assembly of oxidase subunits together with their accompanying metallochaperone interactions.

Three main experimental approaches were taken to gain insight into the COX assembly pathway, heavily relying on the use of mild, non-destructive techniques to preserve weak protein interactions. Initially, intermediary complexes and associations were identified using gel electrophoresis in combination with Western blot analysis. In a second step, we selectively co-immunoprecipitated and enriched these complexes, to confirm specific interactions, and finally we conducted a complexome analysis to extend our view towards all proteins likely involved in oxidase biogenesis. Our data now allow us to follow the assembly/metallation processes for COX, starting from newly synthesized SUI all the way to the final insertion of the holoenzyme into supercomplexes (Fig 5).

We find that COX SUI progresses through at least four intermediate states (I₁-I₄), which are discernible by immunostaining after 2D BN/SDS PAGE and are further confirmed by complexome profiling. From co-migration/association behaviour of COX SUII and SUIII, these two subunits apparently enter the stage only at subcomplex I₃, followed by the addition of SUIV (I₃-I₄), and the subsequent association with respiratory chain complexes I and III into supercomplexes (S_{a-c}; Fig 4). Additionally, we can define subcomplex-specific associations with the *Paracoccus* metallochaperones CtaG and Surf1c (Figs 1 and 4).

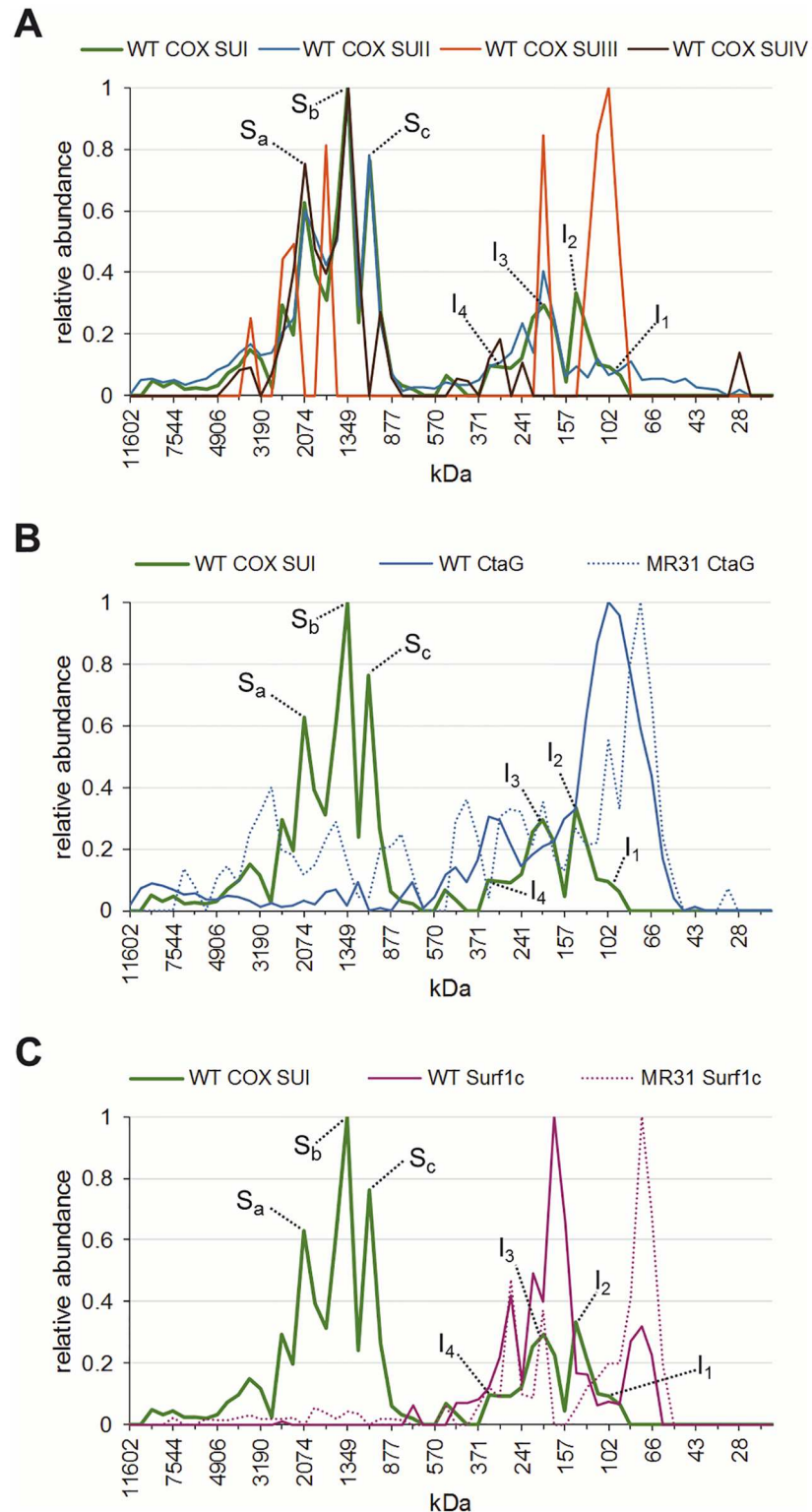


Fig 4. Migration profiles of COX and metallochaperones CtaG and Surf1c obtained by complexome profiling. One-dimensional BN-PAGE of digitonin-solubilized membranes from *P. denitrificans* was analyzed by MS-based complexome profiling. Each panel shows the relative abundance of identified proteins plotted against the apparent molecular mass after BN-PAGE separation. Corresponding heat maps are shown in Fig 3. All profiles are presented as indicated in the legend. (A) Migration profiles of all four COX subunits in a WT

background are shown and the positions of subcomplexes I_{1-4} and supercomplexes S_{a-c} are indicated. (B) Comparison of CtaG migration pattern in membranes prepared from WT or strain MR31, deleted in both COX SUI gene loci, together with the COX SUI WT migration profile. (C) The migration profile of Surf1c is shown for WT and oxidase SUI deletion strain MR31 together with the migration pattern of WT COX SUI.

doi:10.1371/journal.pone.0170037.g004

CtaG is generally believed to be involved in the insertion of a copper ion into the Cu_B site of COX SUI [25, 30], and a direct interaction between these two players was suggested earlier [33]. In addition, we now provide strong evidence for an early association of dimeric CtaG (monomer 21.4 kDa; [54, 58, 59]) with newly synthesized COX SUI (62.4 kDa) to form subcomplex I_1 (≈ 100 kDa; Figs 1 and 4). Based on this finding it is tempting to speculate that metallation of the Cu_B site is the initial step in the assembly line, likely mediated in a co-translational manner [33]. As CtaG remains associated, even though to a minor extent, with later COX assembly intermediates (see Figs 1A and 3A), an additional role as a docking or recruitment factor is conceivable. If the assembly progress is distorted in either mutant background, we speculate that a subfraction of each chaperone (such as in the case of CtaG) does remain attached, for an extended time window, to these subcomplexes. As we also observe an interaction of CtaG with SUII in the pull-down experiments (see Fig 2, $\Delta ctaDI/DII$), we may even ascribe this chaperone the role of a basic scaffold for a COX biogenesis complex, attracting other required chaperones as well. Prior to association of the heme chaperone Surf1c, subcomplex I_1 evolves into subcomplex I_2 , characterized by an extra mass of approximately 40 kDa (in total 140 kDa). This suggests that a so far unknown factor(s) participates in the complex formation.

Surf1c is predominantly found in a larger COX SUI complex, ranging between 160 and 180 kDa which also overlaps with subcomplex I_3 (200 kDa), as confirmed by a shift of migration behaviour in the oxidase SUI deletion strain (Figs 1 and 4). Recruitment of Surf1c may be mediated by both COX SUI and/or CtaG as an interaction between all three proteins was unequivocally confirmed in the WT strain by Co-IP experiments (Fig 2). In prokaryotes,

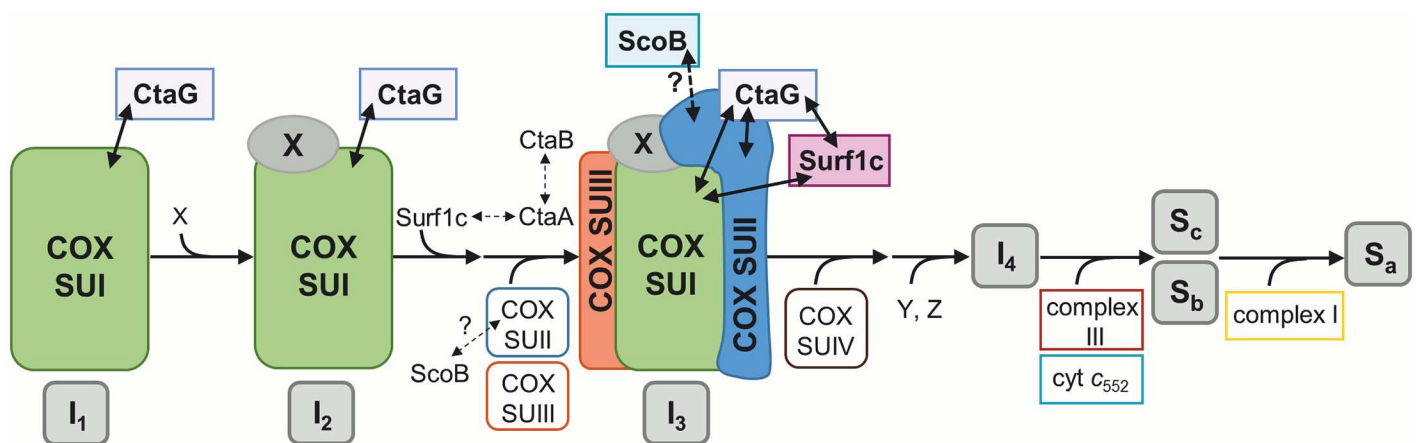


Fig 5. Proposed model of the sequential COX assembly pathway in *P. denitrificans*. COX subunits, respiratory chain complexes and assembly factors are depicted schematically. Direct interactions confirmed by our data are indicated by solid arrows, and presumed interactions by dashed arrows, respectively. Newly translated COX SUI interacts with copper chaperone CtaG to form subcomplex I_1 . This complex evolves into subcomplex I_2 , characterized by an extra mass X of approximately 40 kDa. Formation of subcomplex I_2 is followed by the interaction with Surf1c. Direct interactions between Surf1c and CtaA as well as between CtaB and CtaA are indicated by dashed arrows. After association of Surf1c, COX SUII and SUIII are recruited, leading to formation of subcomplex I_3 . Addition of SUIV leads to formation of the holoenzyme complex, which subsequently associates with subunits of respiratory chain complexes III and I, passing through the supercomplex assembly intermediate I_4 and ultimately ends up in supercomplexes S_c , S_b and S_a .

doi:10.1371/journal.pone.0170037.g005

Surf1c has been strongly linked to the insertion of both heme cofactors into COX SUI, where a significant loss of the heme moiety was observed upon Surf1 deletion [14, 15]: we previously suggested a functional role of Surf1c as both a recruitment factor and as a filter, not only retrieving the heme *a* molecule from its site of synthesis, CtaA, but also discriminating this cofactor over heme *o* before its insertion into SUI [29]. In the COX holoenzyme, the hydrophobic farnesyl side chain of the heme *a*₃ entity is embedded between SUI and SUII [60], suggesting that heme *a* insertion in SUI likely occurs before association with SUII. Consistent with our present data, we conclude that heme insertion takes place in a Surf1c-assisted manner, just prior to formation of subcomplex I₃ and the concomitant association of COX SUII and III. Upon deletion of Surf1c, we observe no significant accumulation of COX SUI assembly intermediates as judged from quantifying relative spot distributions by densitometry (not shown): missing hemylation of SUI seems to go largely unnoticed during further COX biosynthesis steps. As the enzyme activity of isolated oxidase was reported to be highly diminished when purified from a Surf1c deletion mutant, an assembled four-subunit complex obviously does form *in vivo* which, however, lacks activity for the fact that the heme binding sites in SUI remain unpopulated [15, 61]. Yet, an alternative but less efficient heme insertion pathway independent of Surf1c, must be operative, since a fraction of fully cofactor-assembled and therefore active oxidase was reported for Surf1 deletions in all organisms studied so far [15, 23, 24]. In this context heme *a* synthase CtaA may be discussed as immediate alternative donor in the hemylation of COX SUI. Previous studies in *S. cerevisiae* demonstrated a direct interaction between Cox15 (yeast homologue of CtaA) and Shy1p (homologue of Surf1c) in a biogenesis complex and proposed a more direct role of Cox15 as heme *a* insertase [21]. Based on our results, we cannot confirm an association of CtaA with either COX assembly intermediates or Surf1c, however from *in vitro* experiments there is no doubt that Surf1c and CtaA do interact [61]. We therefore conclude that this interaction must be highly transient and evades our present approach. However, based on our complexome profiling (data not shown), it is worth mentioning that Surf1q [15], involved in the delivery of heme *a* to the *ba*₃ quinol oxidase, is not associated with COX assembly intermediates, again emphasizing the specificity of the interaction between the *aa*₃-type terminal oxidase and its corresponding heme chaperone, see [15, 33].

The assembly of COX SUII (28 kDa) and SUIII (30.8 kDa) is observed on the level of subcomplex I₃ (200 kDa). In addition to the COX subunits (121 kDa) this subassembly comprises both the metallochaperones Surf1c (24.6 kDa) and CtaG (21.4 kDa). In this context, CtaG may act as physical mediator for the recruitment of COX SUII, as we observe a direct interaction between CtaG and SUII in our pull-down experiments. Studies with human Sco1 and Sco2 deficient cell lines proposed that Cu_A center formation is required prior to association of SUII with SUI [62]. Our complexome data (see Fig 3) show that ScoB (22.6 kDa) co-migrates with all subcomplexes I₁-I₄, however is mainly found between 60 and 80 kDa, where it is also co-localized with COX SUII when assembly is impaired due to the absence of SUI. This finding may be discussed in support of the above mentioned hypothesis, however metallation of SUII after assembly with SUI cannot be completely ruled out. Our MS data are fully consistent with the earlier observation that neither the second Sco homologue ScoA nor the copper chaperone PCu are involved in this COX biogenesis step [56, 63], clearly confirming that ScoB is the main player in *P. denitrificans*.

Interestingly, we found that prior to association of SUIII this subunit is also present in another complex between 90 and 120 kDa, which accumulates when the main assembly partner COX SUI is missing. We therefore assume that *de novo* translated SUIII is kept in an assembly-competent state, readily available for the assembly process. Co-migration of SUIV is first observed shortly after formation of subcomplex I₃, suggesting that this subunit is added as

the final component to complete formation of the holoenzyme. Importantly COX biogenesis does not stop at this stage, as COX subunits are predominantly found in supercomplexes together with respiratory chain complexes I and III. Therefore, based on complexome profiling, we assume that subcomplex I₄ may represent an early association of functional oxidase with subunit components of complex I.

On the basis of our observations, we suggest a sequential biogenesis model (see Fig 5) for this bacterial COX:

1. COX assembly initiates with SUI, progressing through at least 3 intermediates (I₁-I₃) to complete formation of the holoenzyme.
2. Together with COX SUI, CtaG forms the first subcomplex I₁, suggesting that copper insertion is an early event during oxidase biogenesis possibly independent of heme cofactors.
3. Surf1c enters the assembly line prior to formation of subcomplex I₃ and we hypothesize that Surf1c-mediated heme insertion precedes the addition of SUII and SUIII.
4. Recruitment of SUII may be mediated by assembly factor CtaG, as a direct interaction between SUII and CtaG was observed. Both SUII and SUIII may enter the assembly process in parallel, leading to formation of subcomplex I₃.
5. Assembly proceeds with the addition of SUIV, completing formation of an active four-subunit enzyme.
6. Without significant accumulation in membranes, biogenesis of the holo-form progresses further, leading to the formation of distinct supercomplexes additionally comprising respiratory chain complexes I and III as well as cyt *c*₅₅₂.

Supporting Information

S1 Fig. Separation of solubilized membranes by 2D BN/SDS-PAGE and subsequent silver staining. 140 µg membranes prepared from WT, strain FA2 ($\Delta surf1c$), strain MR31 ($\Delta ctaDI/DII$) or strain ST4 ($\Delta ctaCBGE$) were solubilized with digitonin (digitonin:protein 4:1) and subjected to a first dimension 3.5–18% gradient BN-PAGE. A gel strip was excised and layered on top of a 10% SDS Tricine gel for separation in the second dimension, followed by silver staining. Masses in the first dimension gel were assigned according to (Stroh A, Anderka O, Pfeiffer K, Yagi T, Finel M, Ludwig B, et al. Assembly of respiratory complexes I, III, and IV into NADH oxidase supercomplex stabilizes complex I in *Paracoccus denitrificans*. The Journal of Biological Chemistry. 2004;279(6):5000–7.). Supercomplexes S_a, S_b and S_c run at apparent molecular masses of 1900, 1200 and 900 kDa in the first dimension gel and are separated into their subunit components in the denaturing second dimension SDS gel. Whilst these complexes are present in membranes obtained from WT and strain FA2 (indicated by black bars), they are missing in membranes prepared from strain MR31 and ST4 (expected molecular weight positions of hypothetical supercomplexes S_{a-c} are indicated by grey bars). (PDF)

S2 Fig. Specificity of antisera used in pull-down experiments. In order to check antibody specificity, the following samples were loaded onto a 12% SDS-PAGE and blotted onto nitrocellulose membrane for subsequent Western blot analysis. Blots were probed with the indicated polyclonal rabbit antisera (anti-COX, anti-CtaG (see also Gurumoorthy P, Ludwig B. Deciphering protein-protein interactions during the biogenesis of cytochrome *c* oxidase from *Paracoccus denitrificans*. The FEBS journal. 2015;282(3):537–49), anti-Surf1c and anti-CtaA

(custom immunization, Cambridge Research Biochemicals)) and developed by incubation with protein A-alkaline phosphatase as described in Materials and Methods: M, prestained protein ladder (Thermo Fisher Scientific, 26616); 1, 100 μ g *P. denitrificans* (Pd1222) wildtype membranes; 2, 0.1 μ g purified cytochrome *c* oxidase from *P. denitrificans*; 3, 0.1 μ g purified CtaA from *P. denitrificans* (His₆-tagged construct); 4, 0.1 μ g purified Surf1c from *P. denitrificans* (His₁₀-tagged construct); 5, 0.1 μ g purified CtaG from *P. denitrificans* (His₆-tagged construct). Protein bands at appropriate sizes are indicated by arrows (panel anti-CtaA, lane 3: lower molecular weight bands may represent proteolytic digestion fragments). (PDF)

S3 Fig. Complexome profiles obtained from *P. denitrificans* WT and deletion strains.

Membranes (140 μ g) obtained from *P. denitrificans* WT (A) and deletion strains MR31 (B) and ST4 (C) were solubilized with digitonin with a detergent/protein ratio of 2 g/g and separated by BN-PAGE. The gel lanes were cut into 60 identical slices, trypsin digested and analyzed by liquid chromatography tandem-mass spectrometry. The complexome profiles of respiratory chain complexes and oxidase assembly factors are shown as heat map illustration. For each identified protein, intensity-based absolute quantification (IBAQ) values were normalized to maximum appearance over all 60 slices. Oxidative phosphorylation complexes from bovine heart mitochondria were used for mass calibration. The position of supercomplexes S_{a-c} and assembly intermediates I₁₋₄, as found in the WT strain, is indicated (black bars in WT, grey bars in strain MR31 and ST4). (PDF)

S4 Fig. Migration profiles of respiratory chain complexes. Digitonin-solubilized membranes (140 μ g) from *P. denitrificans* were separated by BN-PAGE and subsequently analyzed by complexome profiling. The average relative abundance value of each complex (taking all its subunits into account) is plotted against the apparent molecular mass in the BN gel. All profiles are coloured as shown in the legend. (A) The migration pattern of respiratory chain complexes I, III and IV, as well as of cyt *c*₅₅₂ is shown in a WT background. Co-migration in the supercomplexes S_{a-c} is indicated, where complex I is only present in supercomplex S_a. Membranes from strain MR31 (B) or strain ST4 (C) do not exhibit supercomplexes. (PDF)

Acknowledgments

We would like to thank Priya Gurumoorthy, Oliver-M. H. Richter and Carolin Werner (Institute of Biochemistry) as well as Volker Zickermann and Andrea Duchêne (Structural Bioenergetics Group, Biochemistry II) for their helpful support of the project. Further we would like to thank Jana Meisterknecht for excellent technical assistance.

Author Contributions

Conceptualization: SS IW BL KMP.

Data curation: SS IW.

Formal analysis: SS IW BL KMP.

Funding acquisition: IW BL KMP.

Investigation: SS IW.

Methodology: SS IW.

Project administration: KMP.

Resources: IW BL KMP.

Supervision: BL KMP.

Validation: SS IW BL KMP.

Visualization: SS IW.

Writing – original draft: SS IW BL KMP.

Writing – review & editing: SS IW BL KMP.

References

1. Kaila VR, Sharma V, Wikstrom M. The identity of the transient proton loading site of the proton-pumping mechanism of cytochrome *c* oxidase. *Biochimica et biophysica acta*. 2011; 1807(1):80–4. doi: [10.1016/j.bbabi.2010.08.014](https://doi.org/10.1016/j.bbabi.2010.08.014) PMID: [20831859](https://pubmed.ncbi.nlm.nih.gov/20831859/)
2. Kaila VR, Verkhovsky MI, Wikstrom M. Proton-coupled electron transfer in cytochrome oxidase. *Chem Rev*. 2010; 110(12):7062–81. doi: [10.1021/cr1002003](https://doi.org/10.1021/cr1002003) PMID: [21053971](https://pubmed.ncbi.nlm.nih.gov/21053971/)
3. Sousa FL, Alves RJ, Ribeiro MA, Pereira-Leal JB, Teixeira M, Pereira MM. The superfamily of heme-copper oxygen reductases: types and evolutionary considerations. *Biochimica et biophysica acta*. 2012; 1817(4):629–37. doi: [10.1016/j.bbabi.2011.09.020](https://doi.org/10.1016/j.bbabi.2011.09.020) PMID: [22001780](https://pubmed.ncbi.nlm.nih.gov/22001780/)
4. Richter O-MH, Ludwig B. Heme Proteins, Cytochrome *c* Oxidase. *Encyclopedia of Metalloproteins*. Springer: Kretsinger Robert H.; Uversky Vladimir N.; Permyakov Eugene A. (Eds.); 2013. p. 939–44.
5. McStay GP, Su CH, Thomas SM, Xu JT, Tzagoloff A. Characterization of assembly intermediates containing subunit 1 of yeast cytochrome oxidase. *The Journal of biological chemistry*. 2013; 288(37): 26546–56. doi: [10.1074/jbc.M113.498592](https://doi.org/10.1074/jbc.M113.498592) PMID: [23897805](https://pubmed.ncbi.nlm.nih.gov/23897805/)
6. Carr HS, Winge DR. Assembly of Cytochrome *c* Oxidase within the Mitochondrion. *Accounts of Chemical Research*. 2003; 36(5):309–16. doi: [10.1021/ar0200807](https://doi.org/10.1021/ar0200807) PMID: [12755640](https://pubmed.ncbi.nlm.nih.gov/12755640/)
7. Soto IC, Fontanesi F, Liu J, Barrientos A. Biogenesis and assembly of eukaryotic cytochrome *c* oxidase catalytic core. *Biochimica et biophysica acta*. 2012; 1817(6):883–97. doi: [10.1016/j.bbabi.2011.09.005](https://doi.org/10.1016/j.bbabi.2011.09.005) PMID: [21958598](https://pubmed.ncbi.nlm.nih.gov/21958598/)
8. Mick DU, Fox TD, Rehling P. Inventory control: cytochrome *c* oxidase assembly regulates mitochondrial translation. *Nat Rev Mol Cell Biol*. 2011; 12(1):14–20. doi: [10.1038/nrm3029](https://doi.org/10.1038/nrm3029) PMID: [21179059](https://pubmed.ncbi.nlm.nih.gov/21179059/)
9. Dennerlein S, Rehling P. Human mitochondrial COX1 assembly into cytochrome *c* oxidase at a glance. *J Cell Sci*. 2015; 128(5):833–7. doi: [10.1242/jcs.161729](https://doi.org/10.1242/jcs.161729) PMID: [25663696](https://pubmed.ncbi.nlm.nih.gov/25663696/)
10. McStay GP, Su CH, Tzagoloff A. Modular assembly of yeast cytochrome oxidase. *Mol Biol Cell*. 2013; 24(4):440–52. doi: [10.1091/mbc.E12-10-0749](https://doi.org/10.1091/mbc.E12-10-0749) PMID: [23266989](https://pubmed.ncbi.nlm.nih.gov/23266989/)
11. Barrientos A, Gouget K, Horn D, Soto IC, Fontanesi F. Suppression mechanisms of COX assembly defects in yeast and human: Insights into the COX assembly process. *Biochimica et biophysica acta*. 2009; 1793(1):97–107. doi: [10.1016/j.bbamcr.2008.05.003](https://doi.org/10.1016/j.bbamcr.2008.05.003) PMID: [18522805](https://pubmed.ncbi.nlm.nih.gov/18522805/)
12. Greiner P, Hannappel A, Werner C, Ludwig B. Biogenesis of cytochrome *c* oxidase—in vitro approaches to study cofactor insertion into a bacterial subunit I. *Biochimica et biophysica acta*. 2008; 1777(7–8):904–11. doi: [10.1016/j.bbabi.2008.04.003](https://doi.org/10.1016/j.bbabi.2008.04.003) PMID: [18445471](https://pubmed.ncbi.nlm.nih.gov/18445471/)
13. Zee JM, Glerum DM. Defects in cytochrome oxidase assembly in humans: lessons from yeast. *Biochem Cell Biol*. 2006; 84(6):859–69. doi: [10.1139/o06-201](https://doi.org/10.1139/o06-201) PMID: [17215873](https://pubmed.ncbi.nlm.nih.gov/17215873/)
14. Smith D, Gray J, Mitchell L, Antholine WE, Hosler JP. Assembly of cytochrome-*c* oxidase in the absence of assembly protein Surf1p leads to loss of the active site heme. *The Journal of biological chemistry*. 2005; 280(18):17652–6. doi: [10.1074/jbc.C500061200](https://doi.org/10.1074/jbc.C500061200) PMID: [15764605](https://pubmed.ncbi.nlm.nih.gov/15764605/)
15. Bundschuh FA, Hoffmeier K, Ludwig B. Two variants of the assembly factor Surf1 target specific terminal oxidases in *Paracoccus denitrificans*. *Biochimica et biophysica acta*. 2008; 1777(10):1336–43. doi: [10.1016/j.bbabi.2008.05.448](https://doi.org/10.1016/j.bbabi.2008.05.448) PMID: [18582433](https://pubmed.ncbi.nlm.nih.gov/18582433/)
16. Mogi T, Saiki K, Anraku Y. Biosynthesis and functional role of haem O and haem A. *Mol Microbiol*. 1994; 14(3):391–8. PMID: [7885224](https://pubmed.ncbi.nlm.nih.gov/7885224/)
17. Barros MH, Carlson CG, Glerum DM, Tzagoloff A. Involvement of mitochondrial ferredoxin and Cox15p in hydroxylation of heme O. *FEBS letters*. 2001; 492(1–2):133–8. PMID: [11248251](https://pubmed.ncbi.nlm.nih.gov/11248251/)

18. Antonicka H, Leary SC, Guercin GH, Agar JN, Horvath R, Kennaway NG, et al. Mutations in COX10 result in a defect in mitochondrial heme A biosynthesis and account for multiple, early-onset clinical phenotypes associated with isolated COX deficiency. *Hum Mol Genet.* 2003; 12(20):2693–702. doi: [10.1093/hmg/ddg284](https://doi.org/10.1093/hmg/ddg284) PMID: [12928484](https://pubmed.ncbi.nlm.nih.gov/12928484/)
19. Antonicka H, Mattman A, Carlson CG, Glerum DM, Hoffbuhr KC, Leary SC, et al. Mutations in COX15 produce a defect in the mitochondrial heme biosynthetic pathway, causing early-onset fatal hypertrophic cardiomyopathy. *Am J Hum Genet.* 2003; 72(1):101–14. doi: [10.1086/345489](https://doi.org/10.1086/345489) PMID: [12474143](https://pubmed.ncbi.nlm.nih.gov/12474143/)
20. Swenson S, Cannon A, Harris NJ, Taylor NG, Fox JL, Khalimonchuk O. Analysis of Oligomerization Properties of Heme a Synthase Provides Insights into Its Function in Eukaryotes. *The Journal of biological chemistry.* 2016; 291(19):10411–25. doi: [10.1074/jbc.M115.707539](https://doi.org/10.1074/jbc.M115.707539) PMID: [26940873](https://pubmed.ncbi.nlm.nih.gov/26940873/)
21. Bareth B, Dennerlein S, Mick DU, Nikolov M, Urlaub H, Rehling P. The heme a synthase Cox15 associates with cytochrome c oxidase assembly intermediates during Cox1 maturation. *Mol Cell Biol.* 2013; 33(20):4128–37. doi: [10.1128/MCB.00747-13](https://doi.org/10.1128/MCB.00747-13) PMID: [23979592](https://pubmed.ncbi.nlm.nih.gov/23979592/)
22. Leigh D. SUBACUTE NECROTIZING ENCEPHALOMYELOPATHY IN AN INFANT. *Journal of Neurology, Neurosurgery, and Psychiatry.* 1951; 14(3):216–21. PMID: [14874135](https://pubmed.ncbi.nlm.nih.gov/14874135/)
23. Zhu Z, Yao J, Johns T, Fu K, De Bie I, Macmillan C, et al. SURF1, encoding a factor involved in the biogenesis of cytochrome c oxidase, is mutated in Leigh syndrome. *Nat Genet.* 1998; 20(4):337–43. doi: [10.1038/3804](https://doi.org/10.1038/3804) PMID: [9843204](https://pubmed.ncbi.nlm.nih.gov/9843204/)
24. Tiranti V, Hoertnagel K, Carrozzo R, Galimberti C, Munaro M, Granatiero M, et al. Mutations of SURF-1 in Leigh disease associated with cytochrome c oxidase deficiency. *Am J Hum Genet.* 1998; 63(6):1609–21. doi: [10.1086/302150](https://doi.org/10.1086/302150) PMID: [9837813](https://pubmed.ncbi.nlm.nih.gov/9837813/)
25. Khalimonchuk O, Bestwick M, Meunier B, Watts TC, Winge DR. Formation of the redox cofactor centers during Cox1 maturation in yeast cytochrome oxidase. *Mol Cell Biol.* 2010; 30(4):1004–17. doi: [10.1128/MCB.00640-09](https://doi.org/10.1128/MCB.00640-09) PMID: [19995914](https://pubmed.ncbi.nlm.nih.gov/19995914/)
26. Mick DU, Wagner K, van der Laan M, Frazier AE, Perschil I, Pawlas M, et al. Shy1 couples Cox1 translational regulation to cytochrome c oxidase assembly. *EMBO J.* 2007; 26(20):4347–58. doi: [10.1038/sj.emboj.7601862](https://doi.org/10.1038/sj.emboj.7601862) PMID: [17882259](https://pubmed.ncbi.nlm.nih.gov/17882259/)
27. Nijtmans LG, Artal Sanz M, Bucko M, Farhoud MH, Feenstra M, Hakkaart GA, et al. Shy1p occurs in a high molecular weight complex and is required for efficient assembly of cytochrome c oxidase in yeast. *FEBS letters.* 2001; 498(1):46–51. PMID: [11389896](https://pubmed.ncbi.nlm.nih.gov/11389896/)
28. Bundschuh FA, Hannappel A, Anderka O, Ludwig B. Surf1, associated with Leigh syndrome in humans, is a heme-binding protein in bacterial oxidase biogenesis. *The Journal of biological chemistry.* 2009; 284(38):25735–41. doi: [10.1074/jbc.M109.040295](https://doi.org/10.1074/jbc.M109.040295) PMID: [19625251](https://pubmed.ncbi.nlm.nih.gov/19625251/)
29. Hannappel A, Bundschuh FA, Ludwig B. Role of Surf1 in heme recruitment for bacterial COX biogenesis. *Biochimica et biophysica acta.* 2012; 1817(6):928–37. doi: [10.1016/j.bbabi.2011.09.007](https://doi.org/10.1016/j.bbabi.2011.09.007) PMID: [21945856](https://pubmed.ncbi.nlm.nih.gov/21945856/)
30. Hiser L, Di Valentin M, Hamer AG, Hosler JP. Cox11p Is Required for Stable Formation of the CuBand Magnesium Centers of Cytochrome c Oxidase. *Journal of Biological Chemistry.* 2000; 275(1):619–23. PMID: [10617659](https://pubmed.ncbi.nlm.nih.gov/10617659/)
31. Khalimonchuk O, Ostermann K, Rodel G. Evidence for the association of yeast mitochondrial ribosomes with Cox11p, a protein required for the Cu(B) site formation of cytochrome c oxidase. *Curr Genet.* 2005; 47(4):223–33. doi: [10.1007/s00294-005-0569-1](https://doi.org/10.1007/s00294-005-0569-1) PMID: [15776235](https://pubmed.ncbi.nlm.nih.gov/15776235/)
32. Thompson AK, Smith D, Gray J, Carr HS, Liu A, Winge DR, et al. Mutagenic analysis of Cox11 of *Rhodospirillum rubrum*: insights into the assembly of Cu(B) of cytochrome c oxidase. *Biochemistry.* 2010; 49(27):5651–61. doi: [10.1021/bi1003876](https://doi.org/10.1021/bi1003876) PMID: [20524628](https://pubmed.ncbi.nlm.nih.gov/20524628/)
33. Gurumoorthy P, Ludwig B. Deciphering protein-protein interactions during the biogenesis of cytochrome c oxidase from *Paracoccus denitrificans*. *FEBS Journal.* 2015; 282(3):537–49. doi: [10.1111/febs.13160](https://doi.org/10.1111/febs.13160) PMID: [25420759](https://pubmed.ncbi.nlm.nih.gov/25420759/)
34. Lode A, Kuschel M, Paret C, Rodel G. Mitochondrial copper metabolism in yeast: interaction between Sco1p and Cox2p. *FEBS letters.* 2000; 485(1):19–24. PMID: [11086158](https://pubmed.ncbi.nlm.nih.gov/11086158/)
35. Nittis T, George GN, Winge DR. Yeast Sco1, a protein essential for cytochrome c oxidase function is a Cu(I)-binding protein. *The Journal of biological chemistry.* 2001; 276(45):42520–6. doi: [10.1074/jbc.M107077200](https://doi.org/10.1074/jbc.M107077200) PMID: [11546815](https://pubmed.ncbi.nlm.nih.gov/11546815/)
36. Stiburek L, Vesela K, Hansikova H, Hulkova H, Zeman J. Loss of function of Sco1 and its interaction with cytochrome c oxidase. *Am J Physiol Cell Physiol.* 2009; 296(5):C1218–26. doi: [10.1152/ajpcell.00564.2008](https://doi.org/10.1152/ajpcell.00564.2008) PMID: [19295170](https://pubmed.ncbi.nlm.nih.gov/19295170/)
37. Thompson AK, Gray J, Liu A, Hosler JP. The roles of *Rhodospirillum rubrum* copper chaperones PCu(A)C and Sco (PrrC) in the assembly of the copper centers of the aa(3)-type and the cbb(3)-type

- cytochrome *c* oxidases. *Biochimica et biophysica acta*. 2012; 1817(6):955–64. doi: [10.1016/j.bbabbio.2012.01.003](https://doi.org/10.1016/j.bbabbio.2012.01.003) PMID: [22248670](https://pubmed.ncbi.nlm.nih.gov/22248670/)
38. Abajian C, Rosenzweig AC. Crystal structure of yeast Sco1. *J Biol Inorg Chem*. 2006; 11(4):459–66. doi: [10.1007/s00775-006-0096-7](https://doi.org/10.1007/s00775-006-0096-7) PMID: [16570183](https://pubmed.ncbi.nlm.nih.gov/16570183/)
 39. Bourens M, Boulet A, Leary SC, Barrientos A. Human COX20 cooperates with SCO1 and SCO2 to mature COX2 and promote the assembly of cytochrome *c* oxidase. *Hum Mol Genet*. 2014; 23(11):2901–13. doi: [10.1093/hmg/ddu003](https://doi.org/10.1093/hmg/ddu003) PMID: [24403053](https://pubmed.ncbi.nlm.nih.gov/24403053/)
 40. Leary SC, Sasarman F, Nishimura T, Shoubridge EA. Human SCO2 is required for the synthesis of CO II and as a thiol-disulphide oxidoreductase for SCO1. *Human Molecular Genetics*. 2009; 18(12):2230–40. doi: [10.1093/hmg/ddp158](https://doi.org/10.1093/hmg/ddp158) PMID: [19336478](https://pubmed.ncbi.nlm.nih.gov/19336478/)
 41. Castresana J, Lübben M, Saraste M, Higgins DG. Evolution of cytochrome oxidase, an enzyme older than atmospheric oxygen. *The EMBO Journal*. 1994; 13(11):2516–25. PMID: [8013452](https://pubmed.ncbi.nlm.nih.gov/8013452/)
 42. de Vries GE, Harms N, Hoogendijk J, Stouthamer AH. Isolation and characterization of *Paracoccus denitrificans* mutants with increased conjugation frequencies and pleiotropic loss of a (nGATCn) DNA-modifying property. *Archives of Microbiology*. 1989; 152(1):52–7.
 43. Raitio M, Wikström M. An alternative cytochrome oxidase of *Paracoccus denitrificans* functions as a proton pump. *Biochimica et Biophysica Acta (BBA)—Bioenergetics*. 1994; 1186(1):100–6. [http://dx.doi.org/10.1016/0005-2728\(94\)90140-6](http://dx.doi.org/10.1016/0005-2728(94)90140-6).
 44. Steinrucke P, Gerhus E, Ludwig B. *Paracoccus denitrificans* mutants deleted in the gene for subunit II of cytochrome *c* oxidase also lack subunit I. *The Journal of biological chemistry*. 1991; 266(12):7676–81. PMID: [1850416](https://pubmed.ncbi.nlm.nih.gov/1850416/)
 45. Lowry OH, Rosebrough NJ, Farr AL, Randall RJ. Protein measurement with the Folin phenol reagent. *The Journal of biological chemistry*. 1951; 193(1):265–75. PMID: [14907713](https://pubmed.ncbi.nlm.nih.gov/14907713/)
 46. Markwell MA, Haas SM, Bieber LL, Tolbert NE. A modification of the Lowry procedure to simplify protein determination in membrane and lipoprotein samples. *Analytical biochemistry*. 1978; 87(1):206–10. PMID: [98070](https://pubmed.ncbi.nlm.nih.gov/98070/)
 47. Wittig I, Braun HP, Schagger H. Blue native PAGE. *Nature protocols*. 2006; 1(1):418–28. doi: [10.1038/nprot.2006.62](https://doi.org/10.1038/nprot.2006.62) PMID: [17406264](https://pubmed.ncbi.nlm.nih.gov/17406264/)
 48. Schagger H. Tricine-SDS-PAGE. *Nature protocols*. 2006; 1(1):16–22. doi: [10.1038/nprot.2006.4](https://doi.org/10.1038/nprot.2006.4) PMID: [17406207](https://pubmed.ncbi.nlm.nih.gov/17406207/)
 49. Stroh A, Anderka O, Pfeiffer K, Yagi T, Finel M, Ludwig B, et al. Assembly of respiratory complexes I, III, and IV into NADH oxidase supercomplex stabilizes complex I in *Paracoccus denitrificans*. *The Journal of biological chemistry*. 2004; 279(6):5000–7. doi: [10.1074/jbc.M309505200](https://doi.org/10.1074/jbc.M309505200) PMID: [14610094](https://pubmed.ncbi.nlm.nih.gov/14610094/)
 50. Heide H, Bleier L, Steger M, Ackermann J, Drose S, Schwamb B, et al. Complexome profiling identifies TMEM126B as a component of the mitochondrial complex I assembly complex. *Cell Metab*. 2012; 16(4):538–49. doi: [10.1016/j.cmet.2012.08.009](https://doi.org/10.1016/j.cmet.2012.08.009) PMID: [22982022](https://pubmed.ncbi.nlm.nih.gov/22982022/)
 51. Strecker V, Kadeer Z, Heidler J, Cruciat CM, Angerer H, Giese H, et al. Supercomplex-associated Cox26 protein binds to cytochrome *c* oxidase. *Biochimica et biophysica acta*. 2016; 1863(7 Pt A):1643–52. doi: [10.1016/j.bbamcr.2016.04.012](https://doi.org/10.1016/j.bbamcr.2016.04.012) PMID: [27091403](https://pubmed.ncbi.nlm.nih.gov/27091403/)
 52. Giese H, Ackermann J, Heide H, Bleier L, Drose S, Wittig I, et al. NOVA: a software to analyze complexome profiling data. *Bioinformatics*. 2015; 31(3):440–1. doi: [10.1093/bioinformatics/btu623](https://doi.org/10.1093/bioinformatics/btu623) PMID: [25301849](https://pubmed.ncbi.nlm.nih.gov/25301849/)
 53. Wittig I, Beckhaus T, Wumaier Z, Karas M, Schagger H. Mass estimation of native proteins by blue native electrophoresis: principles and practical hints. *Mol Cell Proteomics*. 2010; 9(10):2149–61. doi: [10.1074/mcp.M900526-MCP200](https://doi.org/10.1074/mcp.M900526-MCP200) PMID: [20173216](https://pubmed.ncbi.nlm.nih.gov/20173216/)
 54. Carr HS, George GN, Winge DR. Yeast Cox11, a protein essential for cytochrome *c* oxidase assembly, is a Cu(I)-binding protein. *The Journal of biological chemistry*. 2002; 277(34):31237–42. doi: [10.1074/jbc.M204854200](https://doi.org/10.1074/jbc.M204854200) PMID: [12063264](https://pubmed.ncbi.nlm.nih.gov/12063264/)
 55. Hederstedt L. Heme A biosynthesis. *Biochimica et biophysica acta*. 2012; 1817(6):920–7. doi: [10.1016/j.bbabbio.2012.03.025](https://doi.org/10.1016/j.bbabbio.2012.03.025) PMID: [22484221](https://pubmed.ncbi.nlm.nih.gov/22484221/)
 56. Dash BP, Alles M, Bundschuh FA, Richter OM, Ludwig B. Protein chaperones mediating copper insertion into the CuA site of the aa3-type cytochrome *c* oxidase of *Paracoccus denitrificans*. *Biochimica et biophysica acta*. 2015; 1847(2):202–11. doi: [10.1016/j.bbabbio.2014.11.001](https://doi.org/10.1016/j.bbabbio.2014.11.001) PMID: [25445316](https://pubmed.ncbi.nlm.nih.gov/25445316/)
 57. Khalimonchuk O, Rödel G. Biogenesis of cytochrome *c* oxidase. *Mitochondrion*. 2005; 5(6):363–88. <http://dx.doi.org/10.1016/j.mito.2005.08.002> doi: [10.1016/j.mito.2005.08.002](https://doi.org/10.1016/j.mito.2005.08.002) PMID: [16199211](https://pubmed.ncbi.nlm.nih.gov/16199211/)
 58. Banci L, Bertini I, Cantini F, Ciofi-Baffoni S, Gonnelli L, Mangani S. Solution structure of Cox11, a novel type of beta-immunoglobulin-like fold involved in CuB site formation of cytochrome *c* oxidase. *The Journal of biological chemistry*. 2004; 279(33):34833–9. doi: [10.1074/jbc.M403655200](https://doi.org/10.1074/jbc.M403655200) PMID: [15181013](https://pubmed.ncbi.nlm.nih.gov/15181013/)

59. Hannappel A, Bundschuh FA, Greiner P, Alles M, Werner C, Richter OM, et al. Bacterial model systems for cytochrome *c* oxidase biogenesis. *Indian Journal of Chemistry*. 2011; 50A:374–82.
60. Iwata S, Ostermeier C, Ludwig B, Michel H. Structure at 2.8 Å resolution of cytochrome *c* oxidase from *Paracoccus denitrificans*. *Nature*. 1995; 376(6542):660–9. doi: [10.1038/376660a0](https://doi.org/10.1038/376660a0) PMID: [7651515](https://pubmed.ncbi.nlm.nih.gov/7651515/)
61. Hannappel A, Bundschuh FA, Ludwig B. Characterization of heme-binding properties of *Paracoccus denitrificans* Surf1 proteins. *The FEBS journal*. 2011; 278(10):1769–78. doi: [10.1111/j.1742-4658.2011.08101.x](https://doi.org/10.1111/j.1742-4658.2011.08101.x) PMID: [21418525](https://pubmed.ncbi.nlm.nih.gov/21418525/)
62. Williams SL, Valnot I, Rustin P, Taanman JW. Cytochrome *c* oxidase subassemblies in fibroblast cultures from patients carrying mutations in COX10, SCO1, or SURF1. *The Journal of biological chemistry*. 2004; 279(9):7462–9. doi: [10.1074/jbc.M309232200](https://doi.org/10.1074/jbc.M309232200) PMID: [14607829](https://pubmed.ncbi.nlm.nih.gov/14607829/)
63. Gurumoorthy P, Ludwig B. Deciphering protein-protein interactions during the biogenesis of cytochrome *c* oxidase from *Paracoccus denitrificans*. *The FEBS journal*. 2015; 282(3):537–49. doi: [10.1111/febs.13160](https://doi.org/10.1111/febs.13160) PMID: [25420759](https://pubmed.ncbi.nlm.nih.gov/25420759/)